IEEE Access
Multidisciplinary | Rapid Review | Open Access Journal

Received March 17, 2019, accepted April 7, 2019, date of current version May 1, 2019.

Digital Object Identifier 10.1109/ACCESS.2019.2912220

Frequency Domain Analysis of Lossy and Non-Uniform Twisted Wire Pair

YAXIU SUN, (Fellow, IEEE), JIANLI WANG, WENLIANG SONG, AND RUI XUE
School of Information and Communications Engineering, Harbin Engineering University, Harbin 150001, China

Corresponding author: Rui Xue (xuerui0216@hotmail.com)

This work was supported in part by the National Natural Science Foundation of China under Grant 51209055, in part by the China Postdoctoral Science Foundation under Grant 2015T80324, and in part by the Natural Science Foundation of Heilongjiang, China under Grant F2015028.

ABSTRACT In the study of the frequency domain crosstalk for twisted pair, the traditional alternating inversion model is often built under the ideal condition of lossless and uniform media, ignoring the length of the twisted section. This paper focuses on the impact of these non-ideal conditions on crosstalk, applying the cascaded transmission line theory of Paul and McKnight to predict near-end crosstalk (NEXT) of two pairs of twisted wire pair (TWP) which are placed above a perfectly conducting ground or in a cylindrical ideal conductive shell. This paper put forward the non-uniform-media layered connection method (NLCM) to solve the parasitic parameter matrix, taking two layers as an example. Based on the deduced chain parameter matrix and boundary conditions, the exact crosstalk solution is obtained. All theories in this paper are of great significance to the EMC design of high-speed data transmission systems, providing the theoretical support for predicting NEXT within each device or system.

INDEX TERMS Crosstalk, frequency domain analysis, non-uniform-media layered connection method (NLCM), transmission lines, twisted wire pair (TWP).

I. INTRODUCTION

With a noticeable trend towards smaller, lighter and multi-functional electronic equipment, the electromagnetic space within the equipment is greatly reduced, a variety of crosstalk, electromagnetic interference and signal integrity issues caused by the twisted wire pair (TWP) become increasingly serious [1], [2]. Crosstalk is random, but in a deterministic model, crosstalk is essentially accurate [3]. Based on the classical and typical multiconductor-transmission-line (MTL) model, applying the cascaded transmission line theory of Paul and McKnight [4], [5], the simplified alternative inverted twisted pair model was established and has been continuously applied in more complex electromagnetic environment, mathematical and probability model [3], [6].

Spadacini et al. considered the influence of factors related to the pitch non-uniformity of twisted pair on crosstalk [7]. Spadacini et al. predicted the crosstalk caused by non-uniform incident electromagnetic fields of lossless TWP harness above the ground in [8], in which the non-uniform MTL was treated as an equivalent uniform MTL with averaged parasitic parameters. Considering the impracticality of a particular mathematical model, crosstalk was studied based on statistical models in [9]. The above two papers analyzed the influence of insulating coating only via MoM simulation but did not deduce the closed solution under the conditions of non-uniform media. Grassi and Pignari studied the sensitivity of the load to crosstalk by fine tuning the load [10]. The second-order effect, the dual-Slope behavior (crosstalk increases with 40 dB instead of 20 dB per decade), was further analyzed in [11]. The paper [12] proved that the coupling generated by the terminal is dominant, regardless of the number of nodes, compared with the coupling produced by the twisted sections. The paper [6] and [13] analyzed the impact of twist-pitch non-uniformity on crosstalk in twisted wire pairs, but the difference is that the former analyzed whether the random non-uniformity of the twist pitch can reduce crosstalk, and the latter analyzed the effect of pitch error on the level of interference.

Many of the above studies are based on ideal conditions, such as 1) the length of the twisted section is regarded as zero, 2) conductor is ideal, 3) the media surrounding the conductor is lossless and uniform and so on. Which leads to the strong limitations of crosstalk prediction. In particular, the distance

The associate editor coordinating the review of this manuscript and approving it for publication was Andrei Muller.

between the wires in the twisted section changes with the position, resulting in the parasitic parameters are not uniform, and the calculation of the parasitic parameters is complex and relatively difficult in the case of non-uniform media. Chain parameter matrix changes with the parasitic parameters, thus affecting the final crosstalk value solution.

At present, most of the papers still model the twisted pair as the series of parallel and twisted parts, but in the actual derivation and simulation, the twisted length is regarded as zero, only the inversion matrix P represents the twist. Considering the twisted length will be closer to the actual model, and the crosstalk obtained is closer to the actual value.

In this paper, we establish a new model to represent the lossy and non-uniform twisted-wire pairs considering the length of the twisted section, which are commonly used in control circuits, for crosstalk simulations of lossy and non-uniform twisted wire pair in cable using the frequency-domain research.

This paper is outlined as follows. In Section II, the crosstalk model of the twisted wire pair is established. This part include its circuit model, mathematical model and parameter solution. What's the most important is solving the parasitic parameter under the strict restrictions on non-uniform media. In Section III, the NEXT is obtained by deriving the chain parameter matrix and setting the boundary condition. Several simulations in different conditions reported in Section IV assess the computational efficiency of the model and shows the crosstalk intuitively.

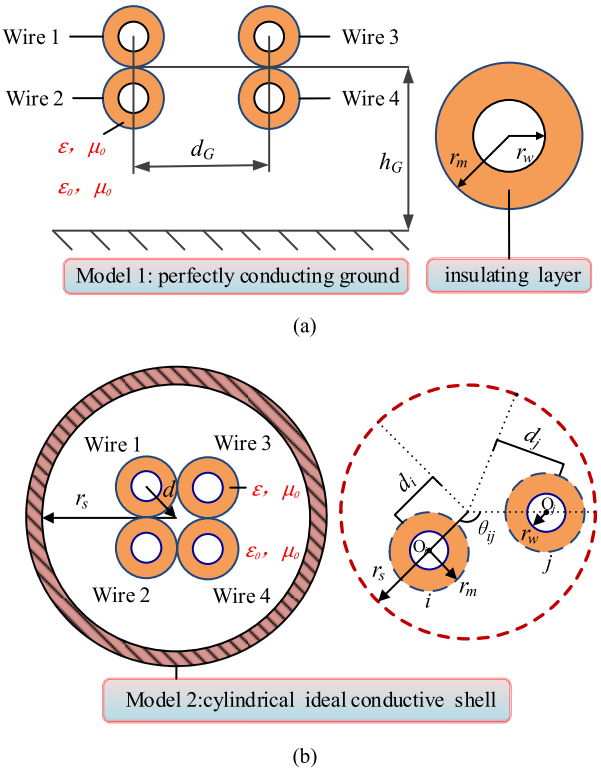

FIGURE 1. New crosstalk circuit model of two pairs of TWPs (cross-sectional view) (a) model 1: Above a perfectly conducting ground (b) model 2: In a cylindrical ideal conductive shell.

II. CROSSTALK MODEL OF THE TWISTED WIRE PAIR

In this paper, we establishe two crosstalk models, as shown in Fig.1. Two pairs of twisted pair with insulating layer are the object of study, which are placed above the perfectly conducting ground (shown in Fig.1 (a)) or in the cylindrical ideal conductive shell (shown in Fig.1 (b)), whose transverse cross section is uniform. The transmission lines are limited to lossy and non-uniform transmission lines, whose conductor is not ideal, the media around the conductor is lossy and is non-uniform.

Since the two wires forming each TWP are wound into a bifilar helix, the cross section of the structure is variable. However, by assuming that relative positions of two TWPs are invariant, the cross-sectional structure can be represented as shown in Fig.1. Wires 1 and 2 in the twisted wire pair are connected to the voltage source Vs. They acts as the aggressor in this configuration. Wires 3 and 4 in the twisted wire pair act as the victim pair. All wires are assumed to have the same radius. The radius of the inner conductor is $r_w = 0.4064mm$, the outer radius of the insulating layer is $r_m = 0.889mm$. The height above ground is $h_G = 3$cm and the horizontal distance between the wires is $d_G = 2$ cm in Fig.1 (a). The inner radius of the conductive shell is $r_s = 1.778mm$. The distance between the ith wire and the center of the shell is d_i and the angle between the ith wire and the jth wire is θ_{ij} in Fig.1 (b). Part of the electric field exists in the region of the lossy insulating media, and the other part is in the free space. All wires have two different dielectric regions, with lossy and non-uniform dielectric parameters:

Insulating layer: ε, μ_0, $\tan\delta$ (loss tangent), $r_w < r < r_m$

Free space: ε_0, μ_0, $r_m < r$ in Fig.1(a), $r_m < r < r_s$ in Fig.1(b).

Complex dielectric constant of insulating layer:

$$\hat{\varepsilon} = \varepsilon - j\varepsilon_p \cong \varepsilon - j\varepsilon\tan\delta = \varepsilon(1 - j\tan\delta) \tag{1}$$

A. Modeling

In this chapter, we establishe the new two-point periodic alternate crosstalk circuit model of twisted pair, the micro-element equivalent circuit model, and applied the specific transmission line equation including the loss parameters.

The new two-point periodic alternate crosstalk circuit model of twisted pair is shown in Fig.2.The excitation source is a boardband frequency signal with $|V_S| = 1$V, internal resistance $R_s = 10\Omega$. The other loads at both ends are set to $R_{x'} = 30\Omega$ (x' is the subscript of each resistance).Each half reverse cycle consists of a parallel section and twisted section, the twisted section includes non-parallel part X_1-X_2, X_2-X_3 and the intersection point p, as shown in Fig.2. The length of the parallel section is l. The length of twisted section is $2l'$, one half of that is l'.

If we take a micro-element in the non-parallel part of every twisted part, the four micro-lines can also be regarded as parallel lines, but the line-line distance varies linearly with

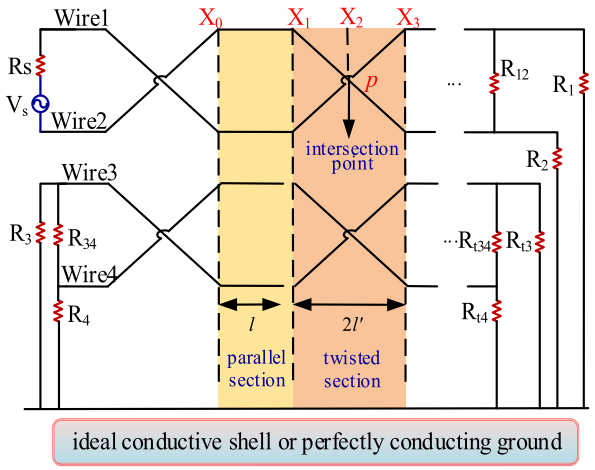

FIGURE 2. New crosstalk circuit model of TWP (longitudinal view).

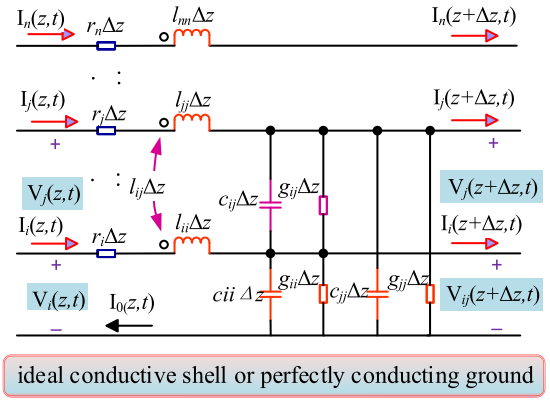

FIGURE 3. The equivalent circuit model of a micro-element Δz.

the position. Therefore, every section can be represented by traditional MTL equivalent circuit model. The model is shown in Fig. 3 (without loss of generality, n is set to 4 here).

The relationship of the transmission line voltages and currents can be determined as follows:

$$\frac{\partial \mathrm{V}_i(z,t)}{\partial z} = -\sum_{k=1}^{4} l_{ik}\frac{\partial \mathrm{I}_k(z,t)}{\partial t} - r\mathrm{I}_i(z,t) \tag{2}$$

$$\frac{\partial \mathrm{I}_i(z,t)}{\partial z} = -\sum_{k=1}^{4} c_{ik}\frac{\partial \mathrm{V}_i(z,t)}{\partial t} + \sum_{i\neq j} c_{ij}\frac{\partial \mathrm{V}_j(z,t)}{\partial t} - \sum_{k=1}^{4} g_{ik}\mathrm{V}_i(z,t) + \sum_{i\neq j} g_{ij}\mathrm{V}_j(z,t) \tag{3}$$

where l_{ii} is the averaged self-inductance of the wire, respectively, and l_{ij} is the averaged mutual inductance between the ith wire and the jth wire, $l_{ij} = l_{ji}$ .Similarly, the capacitance, conductance and resistance have the consistent representations.

Convert the formulas into matrix formula, that is

$$\frac{\partial \mathbf{V}(z,t)}{\partial z} = -\mathbf{L}\frac{\partial \mathbf{I}(z,t)}{\partial t} - \mathbf{RI}(z,t)\,. \tag{4}$$

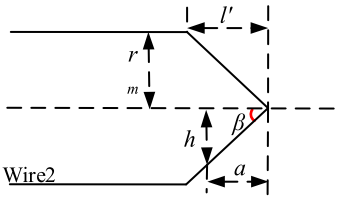

FIGURE 4. New crosstalk circuit model of TWP (longitudinal view).

$$\frac{\partial \mathbf{I}(z,t)}{\partial z} = -\mathbf{C}\frac{\partial \mathbf{V}(z,t)}{\partial t} - \mathbf{GV}(z,t)\,. \tag{5}$$

where the parasitic parameter matrixes **L**, **R**,**C** and **G** are assumed to have the balanced structure perfectly.

B. PARASITIC PARAMETER SOLVING

Next we solve the various parameters in the micro-element circuit model. This is the premise for solving crosstalk.

For the case where the transmission line is placed on the ground plane, detailed reasoning of parasitic parameters in non-uniform media is not performed (the formula can be derived on the basis of the formulas in uniform media given in [16]), only the final simulation result is given directly in section IV. This paper mainly deduces the parasitic parameters in a perfectly conductive cylindrical shell. Parasitic parameters are mainly affected by two factors, one is the varied line-line distance and the other is the non-uniformity of the media.

The line-line distance of cross section varies linearly with the infinitesimal section position, and the angle θ_{ij} changes, resulting in parasitic parameters is not uniform. Each parasitic parameter is related to the position at which the twist portion is located. As seen in Fig. 4 of the illustration of axial wire spacing, $h = a\tan\beta$. Divided the half of the twisted section into m parts, m is relatively large, so the length of each part is $\Delta l^{'} = l^{'}/m$. The similar approach is used in [14].We take the part ith ($a = i\Delta l^{'}$) in the direction, from the intersection to the parallel section. $h_i = i\Delta l^{'}\tan\beta(\tan\beta = r_m/l')$, the distance $d_i = d$ between the ith wire and the center of the shell and the angle θ_{ij} between the ith wire and the jth wire as follows in the parallel section

$$d = \sqrt{2}r_m \tag{6}$$

$$\theta_{ij} = 90^\circ, \quad cos\theta_{ij} = 0\ (ij = 12, 24, 34, 13) \tag{7}$$

$$\theta_{ij} = 180^\circ, \quad cos\theta_{ij} = -1\ (ij = 14, 23) \tag{8}$$

in the twisted section

$$d = \sqrt{h^2 + r_m^2} = \sqrt{(i\Delta l' tan\beta)^2 + r_m^2} \tag{9}$$

$$\theta_{ij} = 180^\circ, \quad cos\theta_{ij} = -1(ij = 14, 23) \tag{10}$$

$$cos\theta_{34} = cos\theta_{12} = 2\left(\frac{h}{d}\right)^2 - 1 \tag{11}$$

$$\theta_{13} = \theta_{24} = 180^\circ - \theta_{34} \tag{12}$$

Since the ideal conductive shell is considered in modeling, we can use the mirror image method [1] to calculate the parasitic inductance matrix for each dielectric

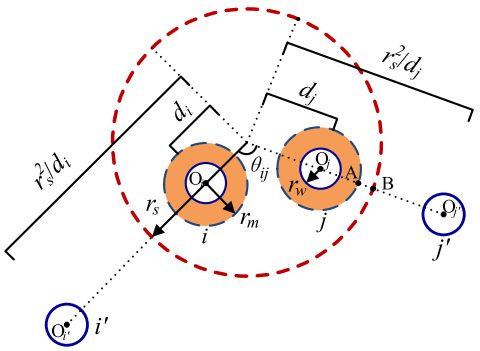

FIGURE 5. Illustration of axial wire spacing.

area and total net inductance matrix, deriving the total net capacitance and conductivity matrix. This method is defined as nonuniform-media layered connection method (NLCM). Take two layers of media for example. Specific instructions are as follows.

The ideal conductive shell can be replaced with a mirror current, located in the radial direction. The distance from the center of the shell to the mirror current i' of current i is r_s^2/d_i, as shown in Fig.5.

For insulating media, $\mu = \mu_0$. Therefore, the averaged inductance is the same as that in the uniform media (free space), and is not affected by the non-uniform media. For the case where the conductor is surrounded by circular insulating media, the dielectric constant of the dielectric around the conductor is non-uniform. So the averaged capacitance, conductance is affected by non-uniform media. Define the averaged inductance matrices of the insulating layer and free space as **L**(INSUL) and **L** (FS) respectively. Similarly, the averaged complex capacitance matrices of the insulating layer and free space are defined as $\hat{C}$(INSUL) and **C**(**FS**) respectively, which can be derived from (13) and (14). If the dielectric constant is real, the capacitance matrix is real, otherwise, is complex.

$$\mathbf{L}(\mathrm{INSUL})\hat{C}(\mathrm{INSUL}) = \mu_0\hat{\varepsilon}\mathbf{E}(4) \tag{13}$$

$$\mathrm{L(FS)C(FS)} = \mu_0\varepsilon_0\mathrm{E}(4) \tag{14}$$

Since the surface $r = r_m$ of the two media is equipotential surface, the total complex capacitor $\hat{C}$ can be regarded as the series capacitance of each region, that is

$$\hat{\mathbf{C}} = \hat{\mathbf{C}}(\mathrm{INSUL})\mathbf{C}(\mathrm{FS})\left[\hat{\mathbf{C}}(\mathrm{INSUL}) + \mathbf{C}(\mathrm{FS})\right]^{-1} \tag{15}$$

Then the net capacitance matrix **C** and net conductance matrix **G** can be obtained directly from the expression of $\hat{C}$.

$$\mathbf{C} = \mathrm{Re}\left[\hat{\mathbf{C}}\right] \tag{16}$$

$$\mathbf{G} = -\omega\mathrm{Im}\left[\hat{\mathbf{C}}\right] \tag{17}$$

From the above analysis we can see that we only need to solve the total parasitic inductance and parasitic inductance of each layer, including **L**, **L**(INSUL) and **L** (FS). The specific steps are as follows.

Define

$$\mathrm{O}_i\mathrm{O}_j = s_{ij}, \quad \mathrm{O}_i\mathrm{A} = s_1, \ \mathrm{O}_i\mathrm{B} = s_1', \tag{18}$$

$$\mathrm{O}_{i'}\mathrm{O}_j = s'', \quad \mathrm{O}_{i'}\mathrm{A} = s_2, \ \mathrm{O}_{i'}\mathrm{B} = s_2' \tag{19}$$

$$l_{ii}\,(\mathrm{INSUL}) = \frac{\mu_0}{2\pi}\ln\left(\frac{r_{mi}}{r_{wi}}\right) + \frac{\mu_0}{2\pi}\ln\left(\frac{\frac{r_s^2}{d_i} - d_i}{\frac{r_s^2}{d_i} - d_i - r_{mi}}\right) \tag{20}$$

$$l_{ii}\,(\mathrm{FS}) == \frac{\mu_0}{2\pi}\ln\left(\frac{r_s - d_i}{r_{mi}}\right) + \frac{\mu_0}{2\pi} \times \ln\left(\frac{\frac{r_s^2}{d_i} - d_i - r_{mi}}{\frac{r_s^2}{d_i} - r_s}\right) \tag{21}$$

$$l_{ii} == \frac{\mu_0}{2\pi}\ln\left(\frac{r_s - d_i}{r_{wi}}\right) + \frac{\mu_0}{2\pi}\ln\left(\frac{\frac{r_s^2}{d_i} - d_i}{\frac{r_s^2}{d_i} - r_s}\right) \tag{22}$$

$$l_{ij}\,(\mathrm{INSUL}) = \frac{\mu_0}{2\pi}\ln\frac{s''s_1}{s_{ij}s_2} \tag{23}$$

$$l_{ij}\,(\mathrm{FS}) = \frac{\mu_0}{2\pi}\ln\frac{s_2s_1'}{s_1s_2'} \tag{24}$$

$$l_{ij} = l_{ji} = \frac{\mu_0}{2\pi}\ln\frac{s''s_1'}{s_{ij}s_2'} \tag{25}$$

where,

$$s_{ij}^2 = d_i^2 + d_j^2 - 2d_id_j\cos\theta_{ij} \tag{26}$$

$$s_1^2 = d_i^2 + \left(d_j + r_{mj}\right)^2 - 2d_i\left(d_j + r_{mj}\right)\cos\theta_{ij} \tag{27}$$

$$\left(s_1'\right)^2 = d_i^2 + r_s^2 - 2d_ir_s\cos\theta_{ij} \tag{28}$$

$$\left(s''\right)^2 = \left(d_j\right)^2 + \left(\frac{r_s^2}{d_i}\right)^2 - 2d_j\left(\frac{r_s^2}{d_i}\right)\cos\theta_{ij} \tag{29}$$

$$s_2^2 = \left(d_j + r_{mj}\right)^2 + \left(\frac{r_s^2}{d_i}\right)^2 - 2\frac{r_s^2}{d_i}\left(d_j + r_{mj}\right)\cos\theta_{ij} \tag{30}$$

$$\left(s_2'\right)^2 = r_s^2 + \left(\frac{r_s^2}{d_i}\right)^2 - 2\frac{r_s^2}{d_i}r_s\cos\theta_{ij} \tag{31}$$

In the model as shown in Fig.1, $r_{wi} = r_{wj} = r_w$, $d_i = d_j = d$, $r_{mi} = r_{mj} = r_m$, so we can get

$$l_{ii}\,(\mathrm{INSUL}) = \frac{\mu_0}{2\pi}\ln\left[\frac{r_m\left(r_s^2 - d^2\right)}{r_w\left(r_s^2 - d^2 - dr_m\right)}\right] \tag{32}$$

$$l_{ii}\,(\mathrm{FS}) = \frac{\mu_0}{2\pi}\ln\left[\frac{\left(r_s^2 - d^2 - dr_m\right)}{r_mr_s}\right] \tag{33}$$

$$l_{ii} = \frac{\mu_0}{2\pi}\ln\left(\frac{r_s^2 - d^2}{r_sr_w}\right) \tag{34}$$

$$l_{ij}\,(\mathrm{INSUL}) = \frac{\mu_0}{2\pi}\ln\sqrt{\frac{a_1a_2}{a_3a_4}} \tag{35}$$

$$l_{ij}\,(\mathrm{FS}) = \frac{\mu_0}{2\pi}\ln\sqrt{\frac{a_3a_5}{a_6a_2}} \tag{36}$$

$$l_{ij} = \frac{\mu_0}{2\pi} \ln\left(\frac{d}{r_s}\sqrt{\frac{d^4 + r_s^4 - 2d^2 r_s^2 \cos\theta_{ij}}{2d^4 - 2d^4\cos\theta_{ij}}}\right). \tag{37}$$

where,

$$a_1 = d^4 + r_s^4 - 2d^2 r_s^2 \cos\theta_{ij} \tag{38}$$
$$a_2 = d^2 + (d + r_m)^2 - 2d\,(d + r_m)\cos\theta_{ij} \tag{39}$$
$$a_3 = (d\,(d + r_m))^2 + r_s^4 - 2d\,(d + r_m)\,r_s^2 \cos\theta_{ij} \tag{40}$$
$$a_4 = 2d^2 - 2d^2\cos\theta_{ij} \tag{41}$$
$$a_5 = d^2 + r_s^2 - 2dr_s\cos\theta_{ij} \tag{42}$$
$$a_6 = d^2 r_s^2 + r_s^4 - 2dr_s^3\cos\theta_{ij} \tag{43}$$

What's more, we can't ignore the skin effect [16] at high frequencies, the current tends to be concentrated on the conductor surface whose thickness is on the order of the skin depth. When the spacing between the wires is wide, the proximity effect is not noticeable, and the current is approximately symmetrical about the bobbin.

The net resistance is,

$$\begin{cases} r = \dfrac{1}{2\pi r_w \sigma \delta}(\Omega/m), & r_w < 2\delta \\ r = \dfrac{1}{2\pi r_w \sigma \delta}(\Omega/m), & r_w > 2\delta \end{cases} \tag{44}$$

the skin depth is,

$$\delta = \frac{1}{\sqrt{\pi f \mu \sigma}} \tag{45}$$

III. RESEARCH OF FREQUENCY DOMAIN SOLUTION

Under the condition that all parasitic parameters are known, we can solve the transmission line equation. In frequency domain, the crosstalk voltage was solved by combining chain parameter matrices and boundary conditions. The paper [15] applied this method in solving crosstalk current and detailed the specific process. The voltage and current of the beginning and that of the terminal are linked through the chain parameter matrix.

A. CHAIN PARAMETER MATRIX SOLUTION

The whole chain parameter matrix links the far-end crosstalk with the near-end crosstalk. Due to the application of parallel line cascade theory, as long as the parallel linear chain parameter matrix can be obtained, the chain parameter matrix of each part and the whole can be obtained by bringing the corresponding parameters.

Convert (4) and (5) to frequency domain equations (46) and (47) [15], [16].That is

$$\frac{d^2}{dz}\hat{\mathbf{V}}(\mathbf{z},\omega) = \hat{Z}(\omega)\,\hat{\mathbf{Y}}(\omega)\,\hat{\mathbf{V}}(z,\omega) \tag{46}$$
$$\frac{d^2}{dz}\hat{\mathbf{I}}(z,\omega) = \hat{\mathbf{Y}}(\omega)\,\hat{\mathbf{Z}}(\omega)\,\hat{\mathbf{I}}(z,\omega). \tag{47}$$

where

$$\hat{\mathbf{Z}}(\omega) = \mathbf{R} + \mathbf{j}\omega\mathbf{L}, \quad \hat{\mathbf{Y}}(\omega) = \mathbf{G} + \mathbf{j}\omega\mathbf{C} \tag{48}$$

Assume that the frequency is fixed, the above equation is coupled, and the basic idea of solving the chain parameter matrix is to decouple the equations by similarity transformations. In order to realize the decoupling, the following modulus conversion is performed

$$\begin{cases} \hat{\mathbf{V}}(z) = \hat{\mathbf{T}}_V \hat{\mathbf{V}}_m(z) \\ \hat{\mathbf{I}}(z) = \hat{\mathbf{T}}_I \hat{\mathbf{I}}_m(z) \end{cases} \tag{49}$$

$$\Longrightarrow \begin{cases} \dfrac{d^2}{dz}\hat{\mathbf{V}}_m(z) = \hat{\mathbf{T}}_V^{-1}\hat{Z}\hat{\mathbf{Y}}\hat{\mathbf{T}}_V\hat{\mathbf{V}}_m(z) = \hat{\gamma}^2\hat{\mathbf{V}}_m(z) \\ \dfrac{d^2}{dz}\hat{\mathbf{I}}_m(z) = \hat{\mathbf{T}}_I^{-1}\hat{\mathbf{Y}}\hat{\mathbf{Z}}\hat{\mathbf{T}}_I\hat{\mathbf{I}}_m(z) = \hat{\gamma}^2\hat{\mathbf{I}}_m(z) \end{cases} \tag{50}$$

Our goal is to obtain diagonalization of $\hat{\mathbf{Z}}\hat{\mathbf{Y}}$ and $\hat{\mathbf{Y}}\hat{\mathbf{Z}}$ by similarity transformations. Since the conductors are identical, the insulating layers have the same thickness and the insulating media has the same dielectric constant, the dielectric surrounding the conductor exhibits a symmetry. As a consequence, $\hat{\mathbf{Z}}\hat{\mathbf{Y}}$ and $\hat{\mathbf{Y}}\hat{\mathbf{Z}}$ are normative matrices that can be diagonalized, that is

$$\hat{\mathbf{T}}_V^{-1}\hat{\mathbf{Z}}\hat{\mathbf{Y}}\hat{\mathbf{T}}_V = \hat{\mathbf{T}}_I^{-1}\hat{\mathbf{Y}}\hat{\mathbf{Z}}\hat{\mathbf{T}}_I = \hat{\gamma}^2 \tag{51}$$

where

$$\hat{\gamma}^2 = \begin{bmatrix} \hat{\gamma}_1^2 & 0 & \cdots & 0 \\ 0 & \hat{\gamma}_2^2 & \ddots & \vdots \\ \vdots & \ddots & \ddots & 0 \\ 0 & \cdots & 0 & \hat{\gamma}_n^2 \end{bmatrix} (n = 4) \tag{52}$$

When the equation is decoupled, $\hat{\Phi}(z)$ represents the chain-parameter matrix of a lossy MTL with length z, we can get

$$\begin{bmatrix} \hat{\mathbf{V}}(z) \\ \hat{\mathbf{I}}(z) \end{bmatrix} = \hat{\mathbf{\Phi}}(z)\begin{bmatrix} \hat{\mathbf{V}} & (0) \\ \hat{\mathbf{I}} & (0) \end{bmatrix} = \begin{bmatrix} \hat{\mathbf{\Phi}}_{11}(z) & \hat{\mathbf{\Phi}}_{12}(z) \\ \hat{\mathbf{\Phi}}_{21}(z) & \hat{\mathbf{\Phi}}_{22}(z) \end{bmatrix}\begin{bmatrix} \hat{\mathbf{V}} & (0) \\ \hat{\mathbf{I}} & (0) \end{bmatrix} \tag{53}$$

where

$$\hat{\mathbf{\Phi}}_{11}(z) = \hat{\mathbf{T}}_V \cosh(\hat{\gamma}z)\,\hat{\mathbf{T}}_V^{-1} \tag{54}$$
$$\hat{\mathbf{\Phi}}_{12}(z) = -\hat{\mathbf{T}}_V \sinh(\hat{\gamma}z)\,\hat{\mathbf{T}}_V^{-1}\hat{\mathbf{Y}}_C^{-1} \tag{55}$$
$$\hat{\mathbf{\Phi}}_{21}(z) = -\hat{\mathbf{Y}}_C\hat{\mathbf{T}}_V sinh(\hat{\gamma}z)\,\hat{\mathbf{T}}_V^{-1} \tag{56}$$
$$\hat{\mathbf{\Phi}}_{22}(z) = \hat{\mathbf{Y}}_C\hat{\mathbf{T}}_V \cosh(\hat{\gamma}z)\,\hat{\mathbf{T}}_V^{-1}\hat{\mathbf{Y}}_C^{-1} \tag{57}$$
$$\hat{Y}_C = \mathbf{Z}^{-1}\hat{\mathbf{T}}_V\hat{\gamma}\hat{\mathbf{T}}_V^{-1} \tag{58}$$

The representation of equations (54)-(58) is equivalent to the equations (15)-(18) in paper [15].

Define chain parameter matrix of semi-periodic as $\hat{\mathbf{\Phi}}(l, l')$. Define chain parameter matrix of Parallel transmission section, non-parallel part of cross section and intersection point respectively as $\hat{\mathbf{\Phi}}(l)$, $\hat{\mathbf{\Phi}}(l')$, $\mathbf{P}$. Take point X_0 and point X_3 as the key points to carry out half cycle research by fully applying the above (53)-(58) on parallel transmission line.

The chain parameter matrix of parallel lines is $\hat{\mathbf{\Phi}}(l)$.

The chain parameter matrix of each part in twisted section is related to the position. Different wire spacing leads to different parasitic parameter matrix, leading to different chain parameter matrix. The chain parameter matrix of part i is $\hat{\mathbf{\Phi}}\left(\Delta l', i\right)$, so the chain parameter matrix of entire twisted section is,

$$\hat{\mathbf{\Phi}}\left(l'\right) = \prod_{i=1}^{m} \hat{\mathbf{\Phi}}\left(\Delta l', i\right) \tag{59}$$

At the intersection, the voltage and the current on the different line of twisted-pair are exchanged, so the point also has the chain parameter matrix, that is,

$$\mathbf{P} = \begin{bmatrix} 0 & 1 & 0 & 0 & 0 & 0 & 0 & 0 \\ 1 & 0 & 0 & 0 & 0 & 0 & 0 & 0 \\ 0 & 0 & 0 & 1 & 0 & 0 & 0 & 0 \\ 0 & 0 & 1 & 0 & 0 & 0 & 0 & 0 \\ 0 & 0 & 0 & 0 & 0 & 1 & 0 & 0 \\ 0 & 0 & 0 & 0 & 1 & 0 & 0 & 0 \\ 0 & 0 & 0 & 0 & 0 & 0 & 0 & 1 \\ 0 & 0 & 0 & 0 & 0 & 0 & 1 & 0 \end{bmatrix} \tag{60}$$

The paper [3] and [17] uses the same definition, based on the assumption that the twist occurs at zero distance.

The Chain parameter matrix of Semi-periodic X_0-X_3 as shown in Fig.2 is:

$$\hat{\mathbf{\Phi}}\left(l, l'\right) = \left[\hat{\mathbf{\Phi}}\left(l'\right)\mathbf{P}\hat{\Phi}\left(l'\right)\right]\hat{\mathbf{\Phi}}(l) \tag{61}$$

For the twisted pair model whose number of half-twist twisted cycle is an integer, assuming that the model contains k full-twist cycles (k can be an integer, or an integer plus 1/2), namely, $2k$ half-twist cycles.

The length of each period is $2\left(l + l'\right)$, N is an integer, then the transmission chain parameters of the whole model is

$$\hat{\mathbf{\Phi}}_T = \begin{cases} \left[\hat{\mathbf{\Phi}}\left(l, l'\right)\right]^{2N}, & k = N \\ \left[\hat{\mathbf{\Phi}}\left(l, l'\right)\right]^{2N+1}, & k = N + 1/2 \end{cases} \tag{62}$$

so

$$\begin{bmatrix} \hat{\mathbf{V}}(z) \\ \hat{\mathbf{I}}(z) \end{bmatrix} = \hat{\mathbf{\Phi}}_T(z) \begin{bmatrix} \hat{\mathbf{V}}(0) \\ \hat{\mathbf{I}}(0) \end{bmatrix}$$
$$\Longrightarrow \begin{bmatrix} \hat{\mathbf{V}}(z) \\ \hat{\mathbf{I}}(z) \end{bmatrix} = \begin{bmatrix} \hat{\mathbf{\Phi}}_{T11}(z) & \hat{\mathbf{\Phi}}_{T12}(z) \\ \hat{\mathbf{\Phi}}_{T21}(z) & \hat{\mathbf{\Phi}}_{T22}(z) \end{bmatrix} \begin{bmatrix} \hat{\mathbf{V}}(0) \\ \hat{\mathbf{I}}(0) \end{bmatrix} \tag{63}$$

B. BOUNDARY CONDITIONS

The chain parameter matrix only gives the relationship between the near-end crosstalk and the far-end crosstalk. In order to get the specific value of the near-end and far-end crosstalk voltage, we must combine the chain parameter matrix with the transmission line boundary conditions.

The load is set to be strictly balanced. As a matter of fact, the existence of load imbalance and load difference will have a significant impact on crosstalk. For the model given in Fig. 2, according to Kirchhoff's law, the initial boundary condition matrix equation is obtained, that is

$$\hat{\mathbf{I}}(0) = \mathbf{A}\hat{\mathbf{V}}(0) + \hat{\mathbf{I}}_s \tag{64}$$

where

$$\mathbf{A} = \begin{bmatrix} -\frac{1}{R_s} & \frac{1}{R_s} & 0 & 0 \\ \frac{1}{R_s} & -\frac{1}{R_s} & 0 & 0 \\ 0 & 0 & \frac{R34 + R_3 + R_4}{R_{34}(R_3 + R_4)} & -\frac{R34 + R_3 + R_4}{R_{34}(R_3 + R_4)} \\ 0 & 0 & -\frac{R34 + R_3 + R_4}{R_{34}(R_3 + R_4)} & \frac{R34 + R_3 + R_4}{R_{34}(R_3 + R_4)} \end{bmatrix} \tag{65}$$

$$\hat{\mathbf{I}}_s = \begin{bmatrix} \frac{\hat{V}_s}{R_s} & \frac{\hat{V}_s}{R_s} & 0 & 0 \end{bmatrix}^T \tag{66}$$

The terminal boundary condition matrix equation is

$$\hat{\mathbf{V}}(z) = \mathbf{Z}_L\hat{\mathbf{I}}(z) \tag{67}$$

where

$$\begin{aligned} \mathbf{Z}_L &= diag\left(Z_{L11}, Z_{L22}, Z_{L33}, Z_{L44}\right) \\ Z_{L11} &= \frac{\mathrm{R_{12}R_1}}{\mathrm{R_{12} + R_1 + R_2}}, \quad Z_{L22} = \frac{\mathrm{R_{12}R_2}}{\mathrm{R_{12} + R_1 + R_2}} \\ Z_{L33} &= \frac{\mathrm{R_{t34}R_{t3}}}{\mathrm{R_{t34} + R_{t3} + R_{t4}}}, \quad Z_{L44} = \frac{\mathrm{R_{t34}R_{t4}}}{\mathrm{R_{t34} + R_{t3} + R_{t4}}} \end{aligned} \tag{68}$$

Take the boundary equation into equation (53) for solution, voltage sources can be cast into closed form as

$$\begin{cases} \hat{\mathbf{V}}(0) = \mathbf{M}^{-1}\mathbf{N}\hat{\mathbf{I}}_s \\ \hat{\mathbf{V}}(z) = \left[\left(\hat{\mathbf{\Phi}}_{T11}(z) + \hat{\mathbf{\Phi}}_{T12}(z)\mathbf{A}\right)\mathbf{M}^{-1}\mathbf{N} + \hat{\mathbf{\Phi}}_{T12}(z)\right]\hat{\mathbf{I}}_s \end{cases} \tag{69}$$

where

$$\begin{aligned} \mathbf{M} = &\left(\hat{\mathbf{\Phi}}_{T11}(z) + \hat{\mathbf{\Phi}}_{T12}(z)\mathbf{A}\right) \\ &- \left(\mathbf{Z}_L\hat{\mathbf{\Phi}}_{T21}(z) + \mathbf{Z}_L\hat{\mathbf{\Phi}}_{T22}(z)\mathbf{A}\right) \end{aligned} \tag{70}$$

$$\mathbf{N} = \mathbf{Z}_L\hat{\mathbf{\Phi}}_{T22} - \hat{\mathbf{\Phi}}_{T12}(z) \tag{71}$$

IV. SIMULATION VERIFICATION

This section covers the validation of the above methods and the simulation results of crosstalk based on the proposed model.

Before simulating the model established in this paper, we should first verify the correctness of the theoretical derivation and crosstalk solving methods in this paper. We use the method in this paper to simulate the model in paper [3] (shown in Fig.6), based on the same simulation conditions. The simulation result are shown in Fig.7. Comparing it with the simulation results in paper [3] (shown in Fig.8), it is found that these curves achieve a good fit, which proves that the theoretical derivation and method of this paper is correct.

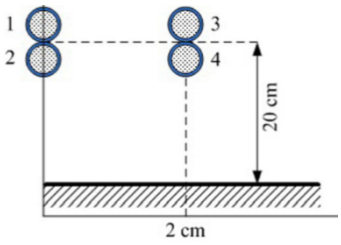

FIGURE 6. Two parallel twisted wires pairs above perfect ground in paper [3].

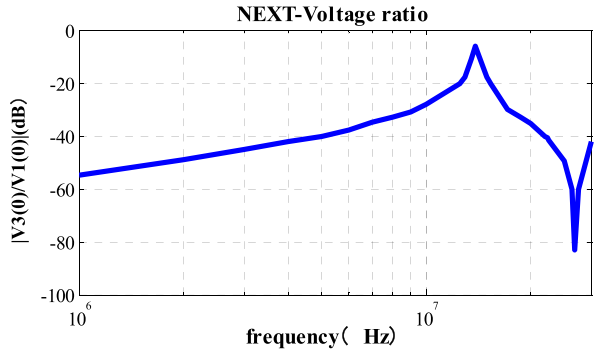

FIGURE 7. The results simulated by the method of this paper of two parallel twisted wires pairs above perfect ground in paper.

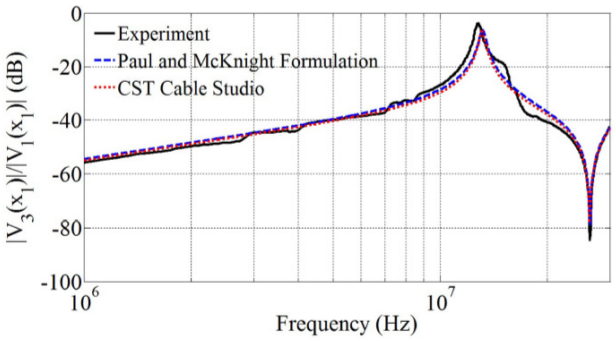

FIGURE 8. Simulation results of two parallel twisted wires pairs above perfect ground in paper [3].

Next, in this section, we simulate the two proposed models and obtain the following result under various conditions, including the near end crosstalk-differential mode (NEXT-DM) voltage value $|V3(0) - V4(0)|$ of disturbed TWP and the NEXT-voltage ratio $|V3(0)/V1(0)|$ of the resulting induced voltage V3 (0) and the voltage V1 (0) .Without loss of generality, the bundle under analysis is composed of two TWPs as shown in Fig. 1, and is characterized by the following data: $\varepsilon = 3.5\varepsilon_0$, $\tan\delta = 0.02$, $l = 0.75$cm, $l' = 0.25cm$. The twisted pair consists of N =50 loops.

A. MODEL 1 ABOVE A PERFECTLY CONDUCTING GROUND IN FIG.1(A)

1) IMPACT OF MEDIA NON-UNIFORMITY ON CROSSTALK

The NEXT-ratio of the resulting induced voltage V3(0) of the victim wire 3 and V1(0) of the transmitting wire 1 in Fig. 1(a) is shown in Fig. 9. When the frequency is less than 100MHz,

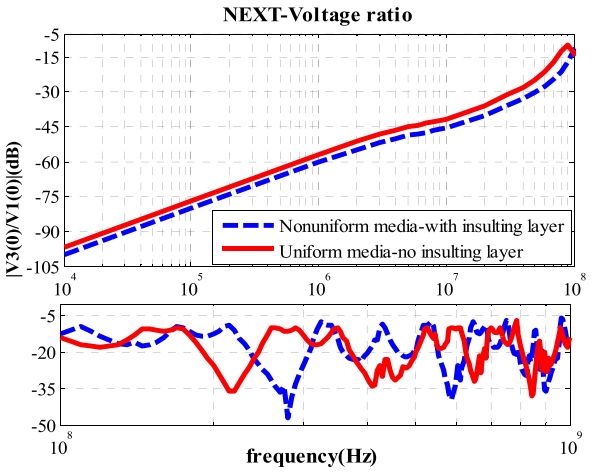

FIGURE 9. NEXT-voltage ratio of lossy TWP above a perfectly conducting ground.

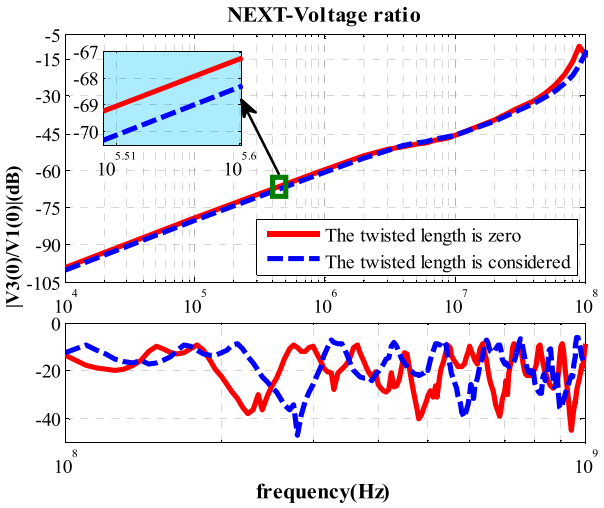

FIGURE 10. NEXT-voltage ratio of lossy and non-uniform TWP above a perfectly conducting ground.

the dashed line is higher than the solid line so that using good insulating materials can effectively suppress crosstalk.

2) IMPACT OF THE TWISTED LENGTH ON CROSSTALK

Twisted pair is set to lossy and non-uniform. We only consider the impact of the twisted length $2l'$ on crosstalk. The curve of voltage ratio as shown in Fig. 10. When the TWP does not resonate, the dashed line is close to the solid line, but the dashed line is slightly higher than the solid line 1dB.

B. MODEL 2 IN A CYLINDRICAL IDEAL CONDUCTIVE SHELL IN FIG.1(B)

1) IMPACT OF LOSSY MEDIA AND TWISTED LENGTH ON CROSSTALK IN BARE TWP

This part ignores the insulation, turns free space into lossy atmospheric space with conduction loss only. Set the atmospheric conductivity $\sigma_0 = 10^{-6}$.

As shown in Fig.11, if only the conduction loss is considered, the dielectric dissipation factor is crucial at frequency

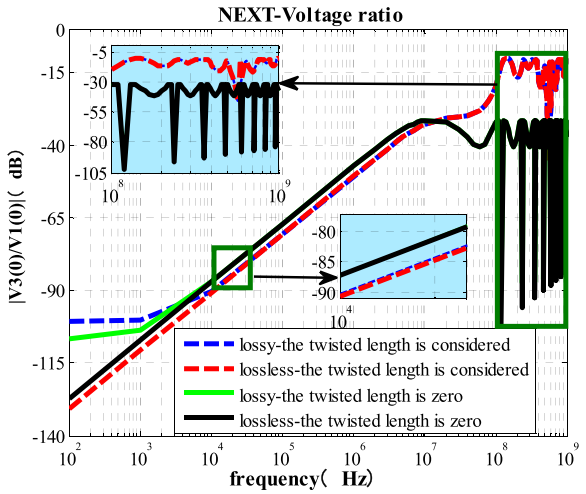

FIGURE 11. NEXT-voltage ratio of uniform TWP in a cylindrical ideal conductive shell.

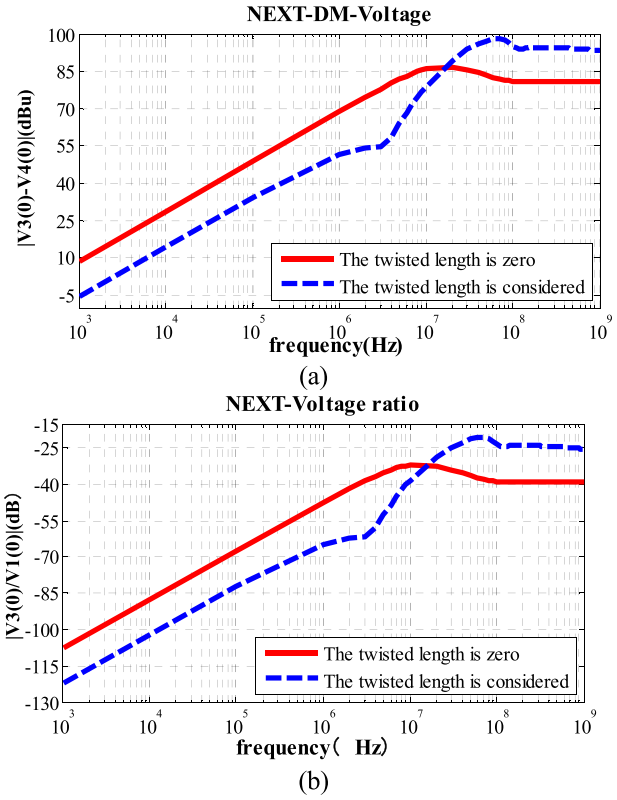

FIGURE 12. NEXT of lossy and non-uniform TWP in a cylindrical ideal conductive shell (a) voltage value (b) voltage ratio.

below 10 kHz. The conduction loss has a significant impact crosstalk at low frequencies. At other frequencies, the curves of lossless media and lossy media tend to be consistent. In addition, the crosstalk ratio of TWP that takes into account twisted length is 3dB smaller than that of TWP regards twisted length as zero, which virtually increases the interference in the magnetic field. When the frequency is higher than 10MHz, considering the twisted length reduces twist resonance phenomenon but increases the crosstalk.

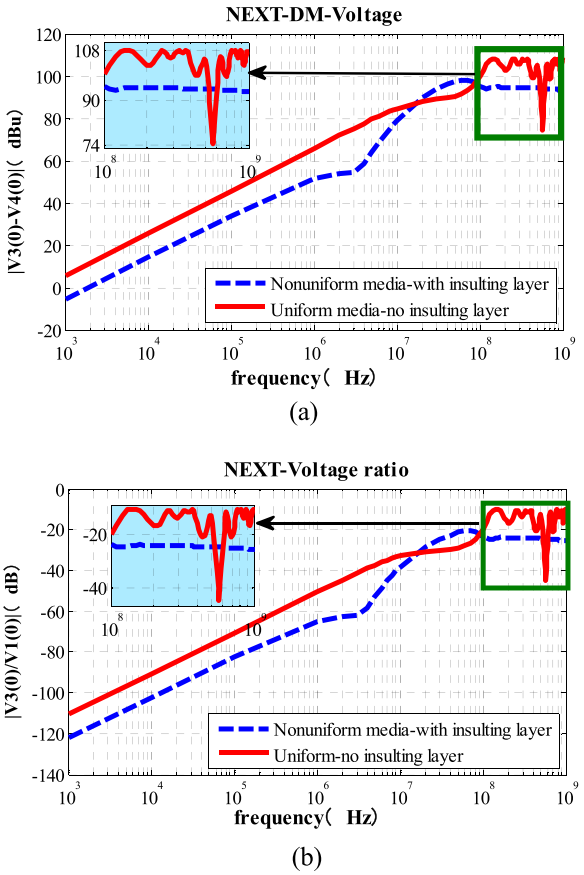

FIGURE 13. NEXT of lossy TWP in a cylindrical ideal conductive shell (a) voltage value (b) voltage ratio.

In practice, the wire usually has an insulating layer, its conductivity is less than 10^{-8}. The greater the frequency, the greater the polarization loss so that conduction loss is Weakened. Thus, the polarization loss is far greater than the conduction loss. Moreover, the series complex capacitance of the double-layer dielectric weakens the loss to a certain degree. So the dielectric loss hardly affects the crosstalk of shield TWPs.

2) IMPACT OF THE TWISTED LENGTH ON CROSSTALK

Predictions of differential crosstalk voltage and crosstalk voltage ratio are plotted in Fig. 12. Comparing the results in Fig. 12 with the aforementioned results in Fig. 10 (above on the earth) , it is obvious that the crosstalk is less when the twisted length is taken into account than when the twisted length is taken as zero, regardless of whether the TWPs are in model 1 or model 2. But the latter is more sensitive to twisted length. The twisted length is considered to be zero, virtually increasing mutual inductance between TWPs, which is more obvious to model 2.

3) IMPACT OF THE MEDIA NON-UNIFORMITY ON CROSSTALK

Obviously, crosstalk with insulation is less than that without insulation at the frequencies below 10MHz, which is consistent with the general physical laws. The curves when the TWP in the conductive shell are more or less different

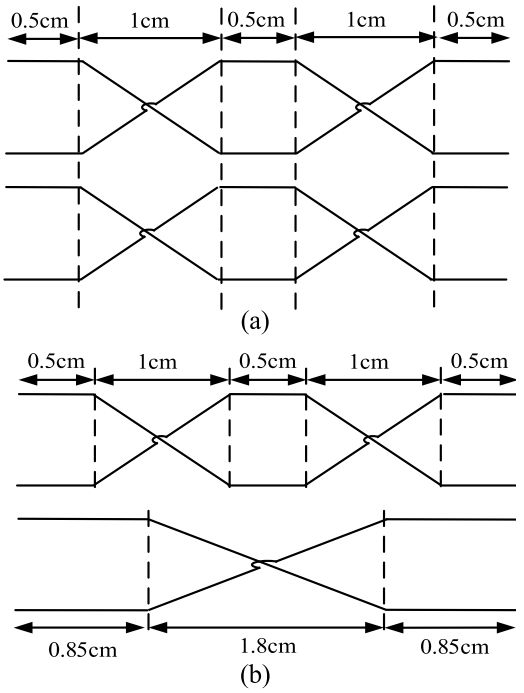

FIGURE 14. TWPs of the same length (a) uniform twist cycle (b) nonuniform twist cycle.

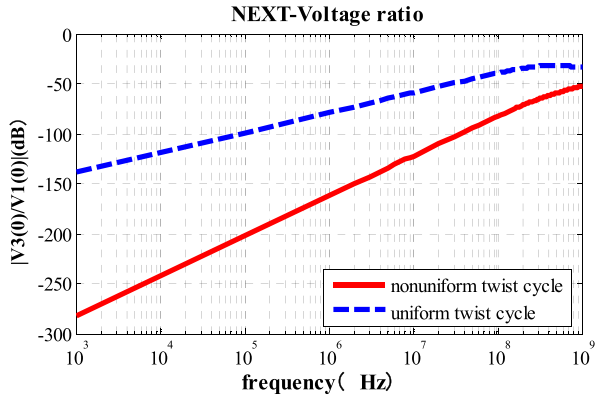

FIGURE 15. NEXT of lossy TWP in a cylindrical ideal conductive shell.

from the curves when the TWP above the earth, as shown in Fig.13.

With the increase of frequency above 10MHz, for the non-uniform TWP, the curves of crosstalk voltage and voltage ratio tend to be fixed, however, for the uniform TWP, the curves of voltage and voltage ratio is oscillating. That is, the insulated wire in the ideal shielding layer can avoid the distortion resonance phenomenon in a certain frequency range. In addition, by introducing the electromagnetic parameters of the insulating medium, the anti-interference performance of different materials can be compared.

4) IMPACT OF THE NON-UNIFORMITY TWIST CYCLE ON CROSSTALK

We artificially set transmission line models with uniform twist cycles and non-uniform twist cycles, which have the same length of 3.5cm, as shown in Fig.14. As can be seen from Fig.15, in the case of non-uniform twisting, the voltage ratio is no longer increased by 20 dB/decade, but by 40 dB/decade or more. Moreover, crosstalk in the case of uniform twist cycle is significantly higher than in the case of non-uniform twist cycle.

V. CONCLUSION

Due to the fact that the lossy and non-uniform TWPs model that fit in practical application comparatively has not been yet established, this paper has established two new models to calculate the crosstalk of lossy and non-uniform TWP considering the length of the twisted section, one above a perfectly conducting ground and one in a cylindrical ideal conductive shell. In this process, the nonuniform-media layered connection method (NLCM) is put forward to solve parasitic parameters. We derive the chain parameter matrix of lossy TWP, and obtain the final crosstalk value with the boundary conditions.

The transmission of high-speed data has certain restrictions on the twisted pair. The method presented in this paper can find important applications in the design of twisted pair in high-speed data transmission systems, such as the following configurations: wire width, insulation material, insulation thickness and layers. In particular, the method NLCM can be widely used to solve the parasitic parameters in electric field with complex structure and multi-dielectric media with high precision. The new crosstalk model is more realistic and can accurately calculate the crosstalk value. It can be used as a theoretical guide for similar problems in wire bundling and crosstalk solving.

REFERENCES

[1] C. R. Paul, *Introduction to Electromagnetic Compatibility*, 2nd ed. New York, NY, USA: Wiley, 2006.

[2] X. Zhang, *Research on Calculation of Crosstalk and Field-to-Wire Coupling on Aircraft*. Nanjing, China: Southeast University, Jun. 2017.

[3] A. Shoory, M. Rubinstein, A. Rubinstein, C. Romero, N. Mora, and F. Rachidi, "Application of the cascaded transmission line theory of Paul and McKnight to the evaluation of NEXT and FEXT in twisted wire pair bundles," *IEEE Trans. Electromagn. Compat.*, vol. 55, no. 4, pp. 648–656, Aug. 2013. doi: 10.1109/TEMC.2013.2254716.

[4] C. R. Paul and J. W. McKnight, "Prediction of crosstalk involving twisted pairs of wires-Part I: A transmission-line model for twisted-wire pairs," *IEEE Trans. Electromagn. Compat.*, vol. EMC-21, no. 2, pp. 92–105, May 1979.

[5] R. Paul and J. W. McKnight, "Prediction of crosstalk involving twisted pairs of wires-Part II: A simplified low-frequency prediction model," *IEEE Trans. Electromagn. Compat.*, vol. ECM-21, no. 2, pp. 105–114, May 1979.

[6] G. Bao, D. Su, F. Dai, and W. Gao, "Statistical analysis for crosstalk of twisted-wire pairs with non-uniform pitch," *J. Beijing Univ. Aeronaut. Astronaut.*, vol. 40, no. 2, pp. 193–197, Feb. 2014.

[7] G. Spadacini, D. Bellan, and S. A. Pignari, "Impact of twist non-uniformity on crosstalk in twisted-wire pairs," in *Proc. IEEE Int. Symp. Electromagn. Compat.*, Aug. 2003, pp. 483–488.

[8] G. Spadacini, F. Grassi, F. Marliani, and S. A. Pignari, "Transmission-line model for field-to-wire coupling in bundles of twisted-wire pairs above Ground," *IEEE Trans. Electromagn. Compat.*, vol. 56, no. 6, pp. 1670–1690, Dec. 2014. doi: 10.1109/TEMC.2014.2327195.

[9] G. Spadacini, F. Grassi, and S. A. Pignari, "Field-to-Wire coupling model for the common mode in random bundles of twisted-wire pairs," *IEEE Trans. Electromagn. Compat.*, vol. 57, no. 5, pp. 1246–1254, Oct. 2015. doi: 10.1109/TEMC.2015.2414356.

[10] F. Grassi and S. A. Pignari, "Bulk current injection in twisted wire pairs with not perfectly balanced terminations," *IEEE Trans. Electromagn. Compat.*, vol. 55, no. 6, pp. 1293–1301, Dec. 2013. doi: 10.1109/TEMC.2013.2255295.
[11] R. F. M. van den Brink, "Modeling the dual-slope behavior of in-quad EL-FEXT in twisted pair quad cables," *IEEE Trans. Commun.*, vol. 65, no. 5, pp. 2153–2163, May 2017. doi: 10.1109/TCOMM.2017.2669032.
[12] C. Jullien, P. Besnier, M. Dunand, and I. Junqua, "Advanced modeling of crosstalk between an unshielded twisted pair cable and an unshielded wire above a ground plane," *IEEE Trans. Electromagn. Compat.*, vol. 55, no. 1, pp. 183–194, Feb. 2013. doi: 10.1109/TEMC.2012.2206599.
[13] G. Spadacini, "Numerical assessment of radiated susceptibility of twisted-wire pairs with random nonuniform twisting," *IEEE Trans. Electromagn. Compat.*, vol. 55, no. 5, pp. 956–964, Oct. 2013. doi: 10.1109/TEMC.2012.2235446.
[14] C. R. Paul and M. B. Jolly, "Crosstalk in twisted-wire circuits, Rome air development center," Griffiss AFB, Rome, NY, USA, Tech. Rep. RADCTR-82 286, vol. IV-C, Nov. 1982.
[15] G. Oriti and A. L. Julian, "Application of the transmission line theory to the frequency domain analysis of the motor voltage stress caused by PWM inverters," in *Proc. Conf. Rec. IEEE Ind. Appl. Conf., 39th IAS Annu. Meeting*, Seattle, WA, USA, vol. 3, Oct. 2004, pp. 1996–2002. doi: 10.1109/IAS.2004.1348742.
[16] C. R. Paul, *Analysis of Multiconductor Transmission Lines*, 2nd ed. New York, NY, USA: Wiley, 2008.
[17] F. Distler, G. Gold, K. Thurn, J. Schür, and M. Vossiek, "Crosstalk simulation of multiple insulated twisted pairs based on transmission line theory," in *Proc. IEEE 21st Workshop Signal Power Integrity (SPI)*, May 2017, pp. 1–4.

YAXIU SUN (M'76–SM'81–F'87) was born in Heilongjiang, China, in 1974. She received the B.S. degree in electrical engineering from Northeast Agricultural University, Harbin, China, in 1997, and the M.S. and Ph.D. degrees in power electronics and electric machines and electric apparatus from the Harbin Institute of technology, Harbin, China, in 2004, and 2008, respectively.

From 1997 to 2002, she was an Assistant Engineer with the Electric Furnace Research Institute. From 2009 to 2012, she was a Lecturer with the College of Information & Communication Engineering, Harbin Engineering University. From 2017 to 2018, she was a Visiting Scholar in electrical and computer engineering, University of Kentucky, KY, USA. She is currently an Associate Professor with the College of Information & Communication Engineering, Harbin Engineering University. Her research interests include EMC, McTL, and crosstalk, computational electromagnetic, antennas design, and advanced electromagnetic theory.

JIANLI WANG was born in Shanxi, China, in 1993. She received the B.S. degree in communication engineering from Harbin Engineering University, Harbin, China, in 2016, where she is currently pursuing the M.S. degree in information and communication engineering. Her current research interests include signal integrity and electromagnetic compatibility.

WENLIANG SONG was born in Heilongjiang, China, in 1994. He received the B.S. degree in electronic information engineering from Northeast Agricultural University, Harbin, China, in 2017. He is currently pursuing the M.S. degree in information and communication engineering with Harbin Engineering University. His current research interests include electromagnetic compatibility and computational electromagnetics.

RUI XUE was born in Heilongjiang, China, in 1980. He received the M.S. and Ph.D. degrees in communication engineering and information and communication engineering from Harbin Engineering University, Harbin, China, in 2006, and 2009, respectively. Since 2003, he has been with the College of Information and Communication Engineering, Harbin Engineering University. From 2011 to 2012, he was an Academic Visitor with the Nonlinear Signal Processing Laboratory, University of Melbourne, Australia. He is currently an Associate Professor with the College of Information and Communication Engineering, Harbin Engineering University. His research interests include radio mobile communication systems, satellite communication systems, and satellite navigation and positioning, and include error-correcting codes, high spectral efficiency modulation, coded modulation, and iterative decoding and detection.